Flow Characteristics in Cylindrical Combustion Chamber

Lect. Fouad Alwan Salih
Mechanical Engineering Department, College of Engineering
Al-Mustansiriya University, Baghdad, Iraq

Abstract

Combustion equipment of turbulent flows has usually been developed empirically, with only qualitative guidance from theory. The reason is that, although has relevant processes have long been understood qualitatively, no accurate and economical procedure has been developed for the quantitative prediction of the properties of flame. Because empirical development is expensive and slow, the need for a prediction procedure which would replace physical by computational experiments is very urgent. The studies which are about to describe are mainly intended to test the ability of the present procedure to provide predictions of temperature calculation of turbulent flows with combustion. It is interesting to note that the maximum-temperature isotherm forms a closed loop within the combustion chamber for the fuel velocity ($V_F=V_o$ and $V_F=05\ V_o$). When V_F increased ($V_F=3V_o$) fuel would escape from the chamber without burning.

الخلاصـــــة

تم إجراء دراسة عددية للجريان المتفاعل المضطرب داخل محرق اسطواني. تمت الدراسة العددية من خلال تطوير برنامج ثنائي الأبعاد متناظر الحيز، مستقر، لجريان مضطرب متفاعل لغرف احتراق أسطوانية.تتضمن الدراسة حل المعادلات التفاضلية الجزئية المتمثلة بحفظ الأستمرارية وانتقال الكتلة للهواء والوقود.توزيع درجات الحرارة وخواص حقل الجريان تم الحصول عليها من خلال الحل.

ثلاث حالات تم اعتمادها عند دراسة الموديل الرياضي وهي اختلاف سرعة دخول الوقود الى داخل المحرق حيث تم اعتماد ثلاث سرع ($v_f=v_o$)،($v_f=0.5v_o$)و($v_f=3v_o$)من انتائج المهمة لهذا البحث هي تاثير زيادة سرعة دخول الوقود الى المحرق حيث لوحظ ان هذه الزيادة تؤدي الى الحصول على درجة الحرارة القصوى عند مخرج المحرق مما يؤدي الى اضرار في مناطق مجابهة اللهب ، كما يمكن ملاحظة هروب جزء من الوقود قبل اكتمال عملية الأحتراق.

1. LITERATURE SURVEY

Grobman [1] performed incompressible flow calculations to determine the effects of combustor geometric and operating variables on pressure loss and airflow distribution in tubular combustor.

Tacina and Grobman [2] analyzed the pressure loss and air flow distribution of an annular combustion chamber taken the effect of geometric and flow variables into consideration. NASA [3] a computer program for the analysis of annular gas turbine combustor including fluid flow. Combustion and heat transfer. Sarkawt [4] presented a theoretical investigation of the compressible, steady one-dimensional, turbulent and chemically reacting flow for various geometrical and inlet flow conditions.

Sturgees, Syed and McManus [5] study the mathematical simulation of the practical problems in the gas turbine engine combustion systems. Sokolov [6] describe a mathematical modeling of an annular gas turbine combustore. A mathematical model for the description of axi-symmetric swirled flow with diffusion combustion is based a numerical solution of the Reynolds equation with (K-ε) model of turbulence.

In this paper a numerical simulation of two dimensional steady, elliptic, turbulent reacting flows with combustion using cylindrical polar co-ordinates were studied. The solution will give the distribution of temperature profile for different axial velocity of fuel (CH4) inlet.

2. THE PHENOMENA CONSIDERED

The combustion processes of gas turbines, ram-jets and many types of industrial furnace exhibit the following features:

i. The flow is turbulent, apart from thin regions close to walls.

ii. The flow is steady, apart from the turbulent fluctuations.

iii. The density, and other fluid properties, varies greatly from place to place, mainly in response to temperature changes resulting from combustion.

iv. Recirculation is present in some parts of the combustion chamber.

v. Although fuel may be injected in the form of liquid droplets, these vaporize in a time, which is so short as to be without influence on the main features of the flame.

3. PHYSICALLY-CONTROLLED COMBUSTION IN A CYLINDRICAL CHAMBER

Figure (1) illustrates cylindrical combustion practical equipment. Fuel and air input at one end; exit for combustion products at other; arrangement of the air inlet as an annular orifice surrounding the fuel inlet; adiabatic and impermeable walls; a device for causing the air to enter with a swirling motion; a thick annular "land" between the air and fuel inlets.

Suppose that the fuel is a methan gas (CH4) having a molecular weight equal to (16) and stoichiometric fuel-air ratio equal to (0.058) for complete combustion. The chemical reaction rate will be presumed to be rapid enough for combustion to be controlled by mixing. For given flow conditions, the present model will be used to compute the distribution of temperature and streamline patterns for variable fuel velocity.

4. THE MATHEMATICAL PROBLEM

The cylindrical shape of the chamber favors the use of the cylindrical-polar co-ordinates Fig. (2). In addition to the equations for Ψ:

$$\frac{\partial}{\partial z}\left(\frac{\ell_2}{\rho \ell_1 r}\frac{\partial \Psi}{\partial z}\right)+\frac{\partial}{\partial r}\left(\frac{\ell_1}{\rho \ell_2 r}\frac{\partial \Psi}{\partial r}\right)+\ell_1\ell_2 w=0 \quad \ldots\ldots\ldots\ldots\ldots\ldots\ldots\ldots (1)$$

And *w:*

$$r^2\left\{\frac{\partial}{\partial z}\left(\frac{w}{r}\frac{\partial \Psi}{\partial r}\right)-\frac{\partial}{\partial r}\left(\frac{w}{r}\frac{\partial \Psi}{\partial z}\right)-\frac{\partial}{\partial z}\left(\frac{\ell_2}{\ell_1}r^3\frac{\partial}{\partial z}\left(\frac{M_{eff}{}^{w}}{r}\right)\right)\right\}$$

$$-\frac{\partial}{\partial r}\left(\frac{\ell_1}{\ell_2}r^3\frac{\partial}{\partial z}\left(\frac{M_{eff}{}^{w}}{r}\right)\right)-\ell_1\ell_2 r\frac{\partial}{\partial z}\left(\rho v_3{}^2\right)-r^2\frac{\partial}{\partial z}\left(\frac{v_1{}^2+v_2{}^2}{2}\right)\frac{\partial \rho}{\partial r}$$

$$+r^2\frac{\partial}{\partial r}\left(\frac{v_1{}^2+v_2{}^2}{2}\right)\frac{\partial \rho}{\partial r}-\ell_1\ell_2 r s_w=0 \quad \ldots\ldots\ldots\ldots\ldots\ldots\ldots\ldots\ldots\ldots (2)$$

Further equations governing the conservation of chemical species:

$$\frac{\partial}{\partial z}\left(m_j \frac{\partial \Psi}{\partial r}\right)-\frac{\partial}{\partial r}\left(m_j \frac{\partial \Psi}{\partial z}\right)-\frac{\partial}{\partial z}\left(\Gamma_{j,eff}\frac{\ell_2}{\ell_1} r \frac{\partial m_j}{\partial z}\right)$$

$$\frac{\partial}{\partial r}\left(\Gamma_{j,eff}\frac{\ell_1}{\ell_2} r \frac{\partial m_j}{\partial z}\right)-\ell_1\ell_2 r R_j = 0 \quad \ldots\ldots (3)$$

It was shown that for a gas engaging in simple chemical reaction, with negligible kinetic heating, and in a chamber with walls which are impervious to both heat and matter, h and Φ_{fo} is linearly related as in equation (7, 8):

$$f = \frac{h - h_o}{h_f - h_o} = \frac{\phi_{fo} - \phi_{fo,o}}{\phi_{fo,F} - \phi_{fo,o}} \quad \ldots\ldots (4)$$

Where the subscripts h_o and F stand respectively for the conditions in the entering streams for oxidant and fuel of course, $\phi_{fo,o}$ has the value-$m_{ox/i}$; and $\phi_{fo,F}$ has the value 1. The equations for h and ϕ_{fo} can thus be replaced by a single one for f.

The relationship between f and the various mass fractions is summarized in the following equations:

$$f_{st} = \frac{1}{(1+i)} \quad \ldots\ldots (5)$$

$$h_{st} = \frac{h_f + ih_o}{1+i} \quad \ldots\ldots (6)$$

$$T_{st} = \frac{h_{fu/cp} + T_f + iT_o}{1+i} \quad \ldots\ldots (7)$$

The straight-line relationships between the various quantities include the following:

$$f \le f_{st} : \begin{cases} m_{ox} = (f_{st} - f)/f_{st} \quad \ldots\ldots (8) \\ T = \{T_f (f - f_{st}) + T_{st}(1 - f)\}/(1 - f_{st}) \quad \ldots\ldots (9) \end{cases}$$

It may be noted that in the absence of chemical reaction f is identical to the mass fraction for the fuel.

4-1 Effective Viscosity

For the present calculations, the effective viscosity will be computed from:

$$\mu_{eff} = kD^{2/3} w^{-1/3} \rho 2/3 (m_f v_f^{\ 2} + m_o v_o^{\ 2})^{1/3} \quad \ldots\ldots (10)$$

where k is a constant, D and w are the chamber dimensions (shown in Fig. (1), m denotes a mass flow rate, and the subscripts F and o refer to conditions in the fuel and air inlets respectively. This formula implies, as may be plausibly expected, that:

i. μ_{eff} Increase with increase of local density.

ii. μ_{eff} Increases with increase of fluid kinetic energy conveyed into the chamber by the fuel and air stream.

iii. μ_{eff} Increases with increase in diameter, but diminishes with increase in length.

iv. μ_{eff} When the density is uniform through the combustion chamber, so is The last of these implications is the least likely to be borne out in practice, nevertheless, even a round-sectioned jet emerging into an infinite stagnant atmosphere can be rough characterized by a uniform value of μ_{eff}, so the implication is certainly not absurd.

According to Pun and Spalding (1967) a value of k equal to 0.012 is suitable.

4-2 Boundary Condition

Figure (2) illustrates the domain of integration and the boundary conditions. At both inlets, the radial velocity is taken as zero, and the axial velocity is given uniform values (100 m/sec); from these conditions the corresponding values of ψ and w/r can be readily evaluated. The mixture

fraction f has the value unity at the fuel inlet and zero at the air inlet. The implicit procedure is used for thew near-wall vorticity calculations.

4-3 Numerical Solution

The starting point for the derivation is the general differential equation

$$a_\phi = \left\{ \frac{\partial}{\partial z}(\phi \frac{\partial \Psi}{\partial r}) - \frac{\partial}{\partial r}(\phi \frac{\partial \Psi}{\partial z}) \right\} - \frac{\partial}{\partial z}\left\{ b_\phi \frac{\ell_2 r}{\ell_1} \frac{\partial (c_\phi \phi}{\partial z} \right\} - \frac{\partial}{\partial r}\left\{ b_\phi \frac{\ell_1 r}{\ell_2} \frac{\partial (c_\phi \phi}{\partial r} \right\}$$
$$+ \ell_1 \ell_2 r d\phi = 0 \quad \ldots\ldots (11)$$

ϕ is the dependent variable (Ψ, w, m_j) and the function are obtained from the following table:

ϕ	a_ϕ	b_ϕ	c_ϕ	d_ϕ
m_j	1	$\Gamma_{j,eff}$	1	$-R_j$
w/r	r^2	r^2	μ_{eff}	$-\frac{r}{\ell_1 \ell_2}(\frac{\partial}{\partial z}\left(\frac{v_1^2 + v_2^2}{2}\right)\frac{\partial \rho}{\partial r} - \frac{\partial}{\partial r}\left(\frac{v_1^2 + v_2^2}{2}\right)\frac{\partial \rho}{\partial r}) - r^2 s_w$
Ψ		$\frac{1}{\rho r^2}$	1	-w/r

The integration of the general differential equation (11) over the small control volume to obtain Fig.(3).

$$A_E(\phi_p - \phi_E) + A_w(\phi_p - \phi_w) + A_n(\phi_p - \phi_n) + A_s(\phi_p - \phi_s)$$
$$- B_E(C_{\phi,E}\phi_E - C_{\phi,p}\phi_p) - B_w(C_{\phi,w}\phi_E - C_{\phi,p}\phi_p) - B_N(C_{\phi,N}\phi_N - C_{\phi,p}\phi_p)$$
$$-(B_s(C_{\phi,s}\phi_s - C_{\phi,p}\phi_p) + d_{\phi,p}v_p = 0 \quad \ldots\ldots (12)$$

Here the A's ,B's and v_f are given by equation 13, 14 and 15 respectively:

$$\left.\begin{aligned} A_E &= a_{\phi,p}[(\Psi_{se}-\Psi_{ne})+|\Psi_{se}-\Psi_{ne}|]/2 \\ A_w &= a_{\phi,p}[(\Psi_{nw}-\Psi_{sw})+|\Psi_{nw}-\Psi_{sw}|]/2 \\ A_n &= a_{\phi,p}[(\Psi_{ne}-\Psi_{nw})+|\Psi_{ne}-\Psi_{nw}|]/2 \\ A_s &= a_{\phi,p}[(\Psi_{sw}-\Psi_{se})+|\Psi_{sw}-\Psi_{se}|]/2 \end{aligned}\right\} \quad \ldots\ldots\ldots\ldots\ldots\ldots\ldots \text{(13)}$$

where

$$\Psi_{se} = \frac{\Psi_{SE}+\Psi_E+\Psi_P+\Psi_S}{4}$$

and similar expression may be derived for Ψ_{ne}, Ψ_{nw} and Ψ_{sw} Fig (3).

$$\left.\begin{aligned} B_E &= \frac{b_{\phi,E}+b_{\phi,p}}{8} * \frac{S_{2,N}-S_{2,s}}{S_{1,N}-S_{1,s}} * (r_E + r_{p)} \\ B_w &= \frac{b_{\phi,w}+b_{\phi,p}}{8} * \frac{S_{2,N}-S_{2,s}}{S_{1,p}-S_{1,w}} * (r_w + r_{p)} \\ B_N &= \frac{b_{\phi,N}+b_{\phi,p}}{8} * \frac{S_{1,E}-S_{1,E}}{S_{1,p}-S_{1,p}} * (r_N + r_{p)} \\ B_s &= \frac{b_{\phi,s}+b_{\phi,p}}{8} * \frac{S_{1,E}-S_{1,w}}{S_{1,p}-S_{2,s}} * (r_s + r_{p)} \end{aligned}\right\} \quad \ldots\ldots\ldots\ldots\ldots\ldots \text{(14)}$$

and

$$v_p = r_p * (\frac{S_{1,N}-S_{1,w}}{2})(\frac{S_{2,N}-S_{2,s}}{2}) \quad \ldots\ldots\ldots\ldots\ldots\ldots\ldots\ldots\ldots\ldots\ldots \text{(15)}$$

Equation (12) is the major outcome of our efforts thus for; it provides an algebraic relation between the value of ϕ at a particular node, and the values at the surrounding nodes. There will of course be one such equation for each variable at every interior node in the field.

5. RESULTS AND DISCUSSION

Once the distribution of the mixture fraction is known, the corresponding values of the temperature can be obtained from equations 7, 8 and 9. For A 21*11 uniformly spaced grid we obtained some computed streamline and temperature patterns for cases in which the fuel velocity equals 0.5,1 and 4 times the air velocity at inlet. Evidently the patterns are influenced by changes in velocity, but not in any remarkable way.

Figure (4) and Fig.(5) presents the results of computations for presently the same circumstance but, on this occasion, chemical reaction has been allowed to take place. It can be seen that the streamlines Fig.(4) have been altered as a consequence of the expansion of the gas which is caused by combustion.

It is interesting to note that; whereas the flame envelope (i.e. the maximum-temperature isotherm) forms a closed loop within the combustion chamber for the first two velocity ratios (the fuel velocity equals 0.5 and 1 times the air velocity at inlet). The flame envelope terminates on the wall for the third one Fig.(5).

The latter behavior implies that fuel would escape from the chamber without burning, an event which is usually undesirable.

Figure (6 a,b,c) shows the temperature behavior along the combustor axis for the present model. It can be seen that the location of maximum temperature is variable according to the fuel inlet velocity (vf=0.5vo, vf=vo, vf=3vo).

Figure (7a,b) and Fig.(8) shows the temperature profile at the exit of combustion chamber for (vf=0.5vo, vf=vo, vf=3vo). It can be seen that the temperature value has dropped from the axis of symmetry towards the wall and has a higher temperature values in the axis of symmetry for vf=0.5vo and vf=vo, while the value of maximum temperature Fig.(8) has located at R=2.5 cm for (vf=3vo). These results are in qualitative agreement with experimental observations.

6. REFERENCES

1. Grobman J. S., ***"Comparison of Calculated and Experimental Total Pressure Loss and Air Flow Distribution in Tubular Combuster with Tapered Linear"***, NASA, Memo.11-2-58E, 1959.

2. Tacina R. R., and Grobman J. S., ***"Analysis of Total Pressure Loss and Air Flow Distribution of Annular Gas Turbine Combustor"***, NASA, TN-D5385, 1969.

3. NASA, ***"Computer Program for the Analysis of Annular Combusters"***, Nothern Research and Engineering Corporation Vol.1, N68-17556 and N68-17557, Jan., 1968.

4. Sarkawt R. H., ***"Computer Molding of a Turbojet Combustion Chamber with Distribution Air-Admission"***, M. Sc. Thesis, University of Baghdad, 1990.

5. Sturgees G. J., Syed S. A., and Mc Manus K. R., ***"Importance of Combustor Flow"***, International Journal of Turbo and Jet Engines, Vol.3, 1986, pp.43-55.

6. Sokolv et. Al., ***"Mathematical Modeling of an Annular Gas Turbine Combustor"***, Transactions of the ASME, Vol.117, January, 1995.

7. Versteeg H. K., and Malalasekera W., ***"An Introduction to Computational Fluid Dynamics. The Finite Volume Method"***, Longman Group Ltd., 1995.

8. Spalding D. B., ***"Concentration Fluctuation in a Round Turbulent Free Jet"***, Chem. Eng. Sic., 26, 1971, pp.98.

NOMENCLATURES

Symbol	*Meaning*
$\ell_1 \ell_2$	Metric coefficient associated with co-ordinates
Z,r	Cylindrical polar co-ordinate
w	Vorticity
V_1, V_2, V_3	Components of the velocity
m	Mass fraction
R_j	The rate of creation of species j
f	The mixture fraction
h	The mixture enthalpy
i	The mass of oxidant
T	The temperature
A,B,C	Coefficient in the general substitution formula
S	The physical distance
Greek	
Ψ	The stream function
Γ	Exchange coefficient
ϕ	Dependent variable
Subscript	
o	Entering stream for oxidant
p	Node p which lies in the center of the "tank"
st	Stoichiometric conditions
j	Chemical species
F	Entering stream for fuel
f_o	Conserved property
n,s,e,w	Co-ordinates of the sides of the "tank"
n_e,s_e,n_w,s_w	Co-ordinates of the centers of the "tank"
1,2,3	Pertaining to directions

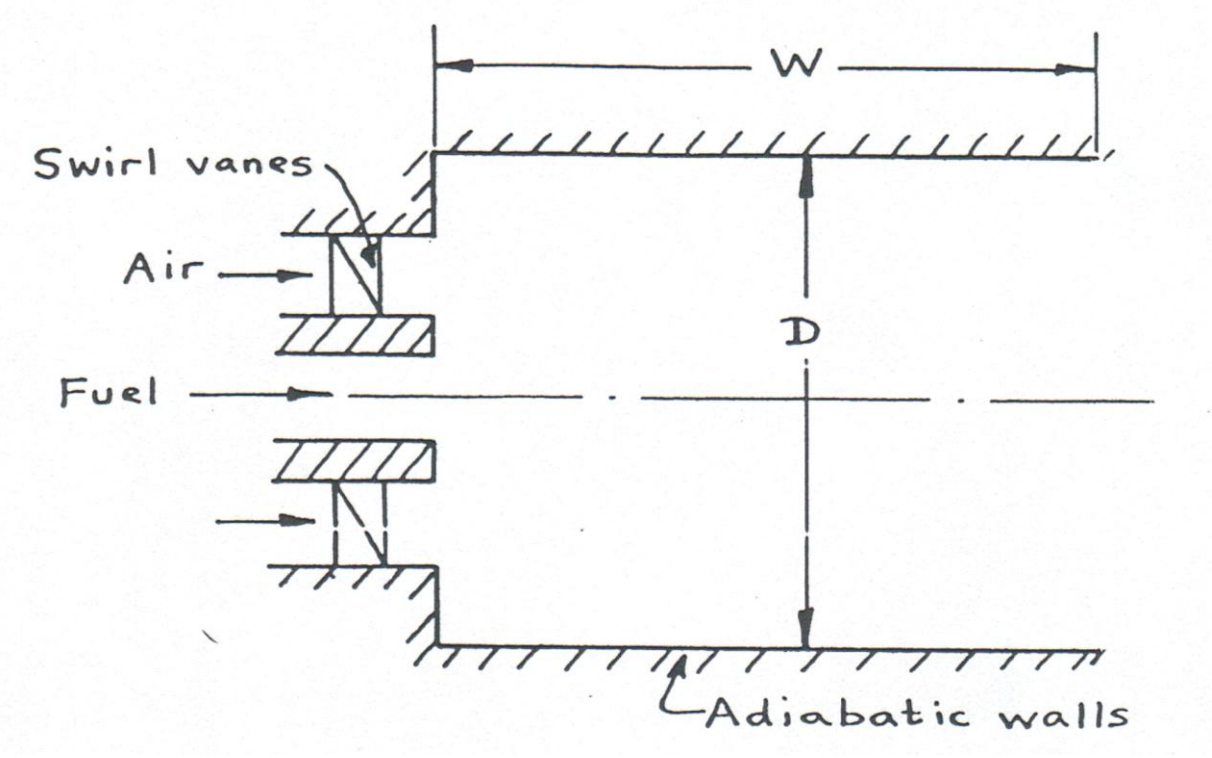

Fig.(1) Cylindrical Combustion Chamber for the Problem of Physically Controlled Processes

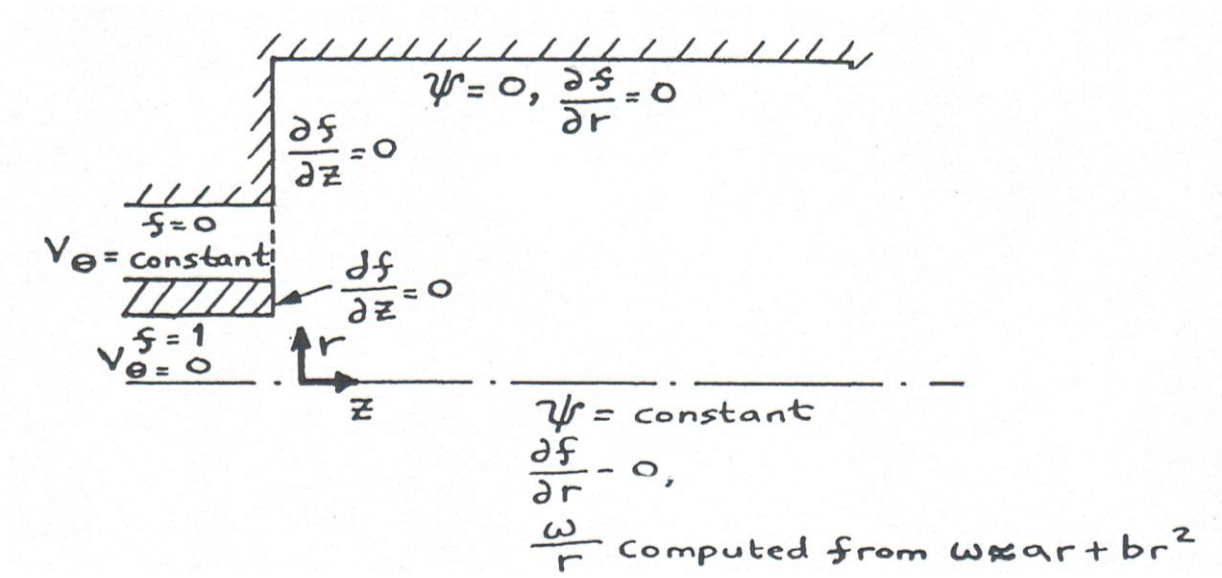

Fig.(2) Illustration of the Domain of Integration and Boundary Conditions for the Cylindrical Combustion Chamber

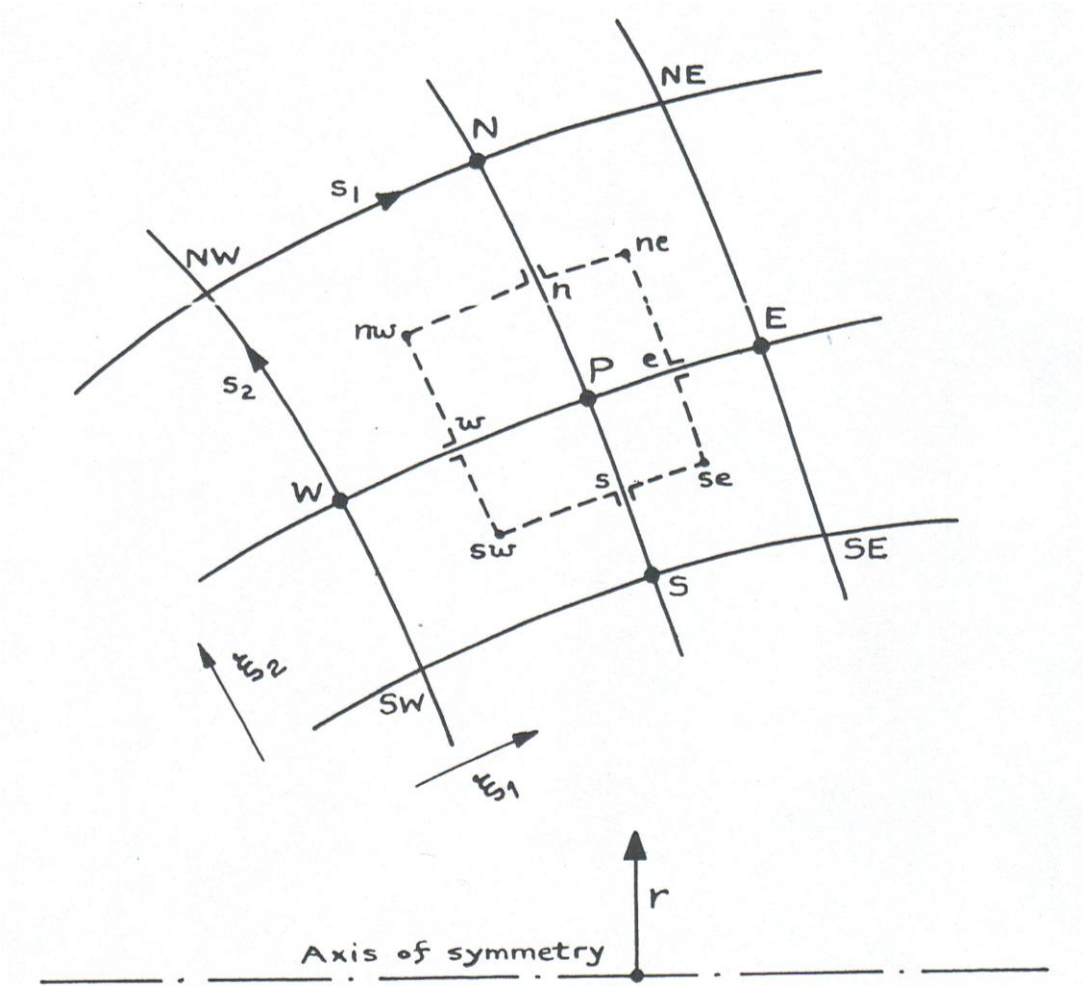

Fig.(3) Illustration of a Portion of the Finite-Difference Grid, the Dotted Lines Enclose the Area of Integration, of 'tank'

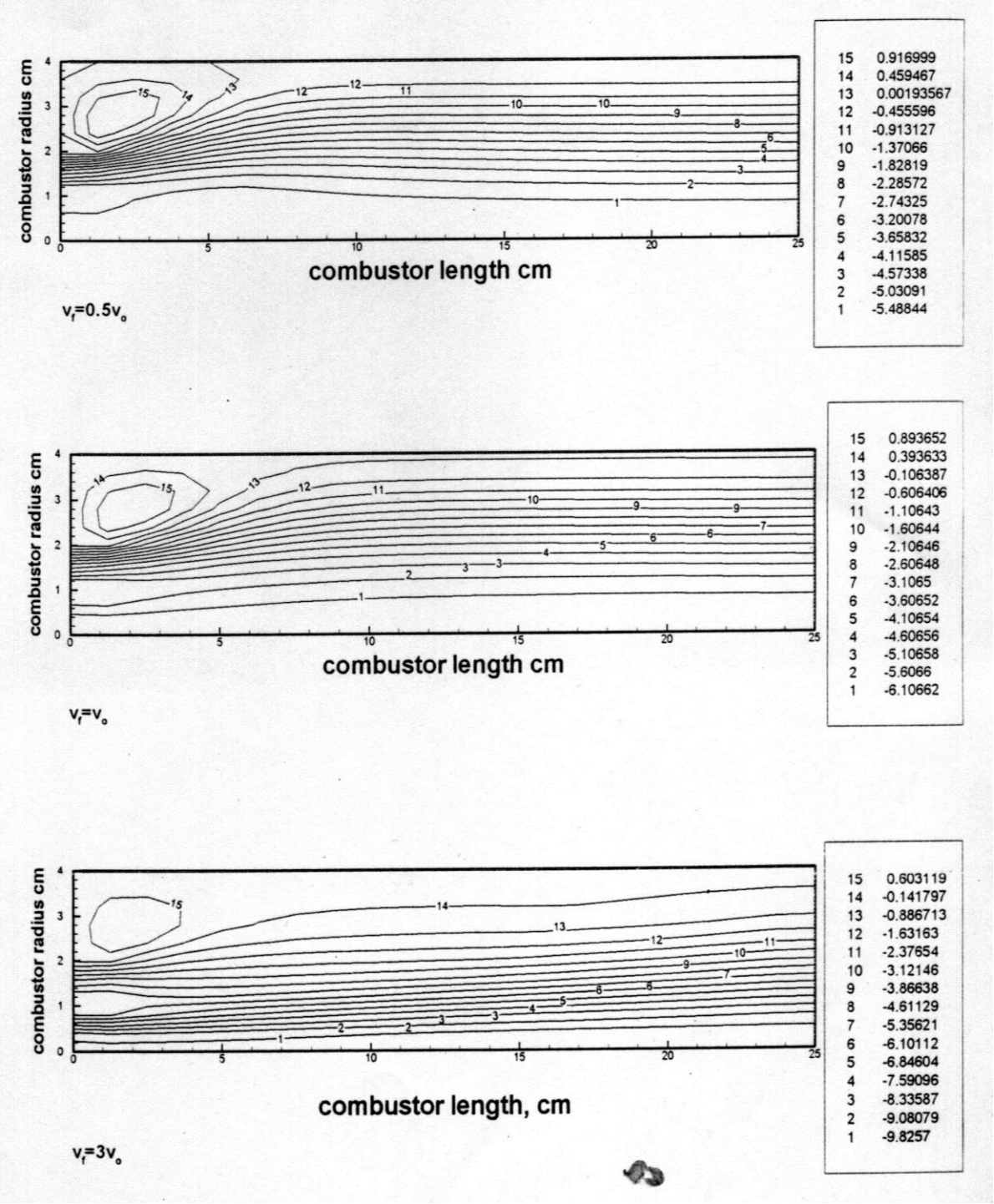

Fig.(4) Stream-Line Patterns for Three Inlet Velocity Ratios, ($v_f=0.5v_o$, $v_f=v_o$, and $v_f=3v_o$), CH_4 Fuel, Air Inlet Temperature=400k

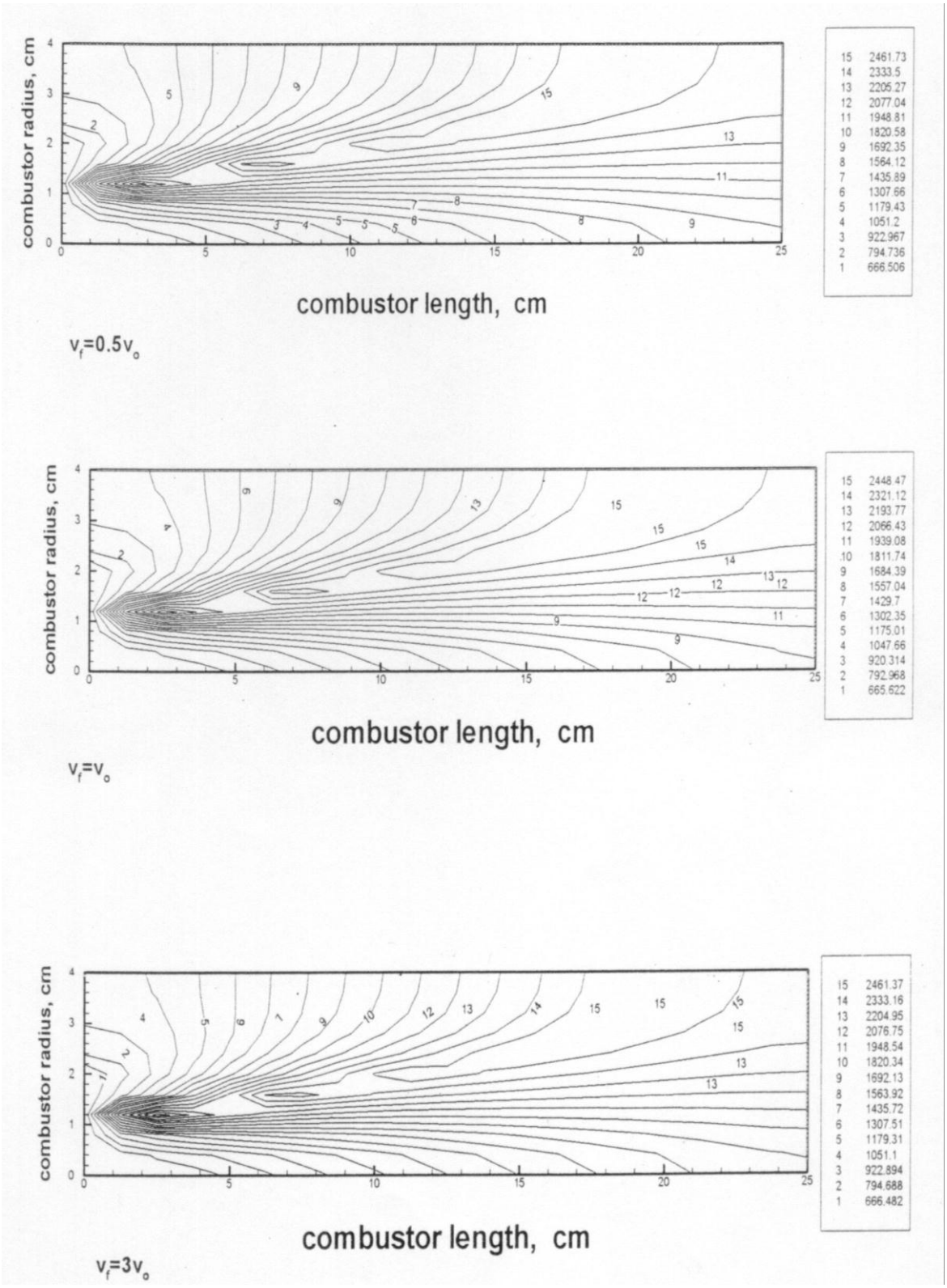

Fig.(5) Temperature Distribution for Three Inlet Velocity Ratios, ($v_f=0.5v_o$, $v_f=v_o$, and $v_f=3v_o$), CH_4 Fuel, Air Inlet Temperature=400k

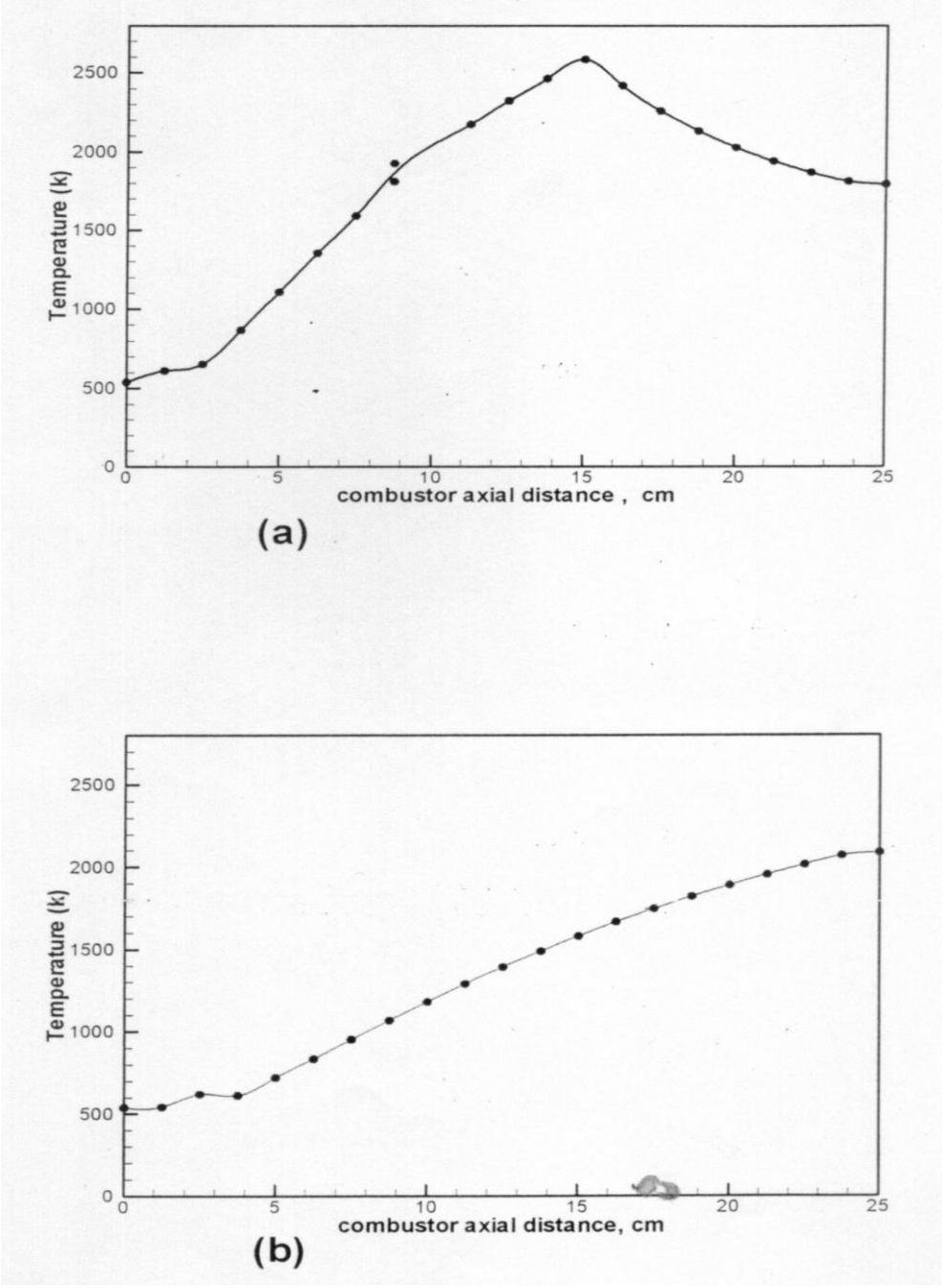

Fig.(6) Temperature Behavior along the Combustion Axis (v_o=40 mls)
(a) $v_f=v_o$ (b) $v_f=3v_o$

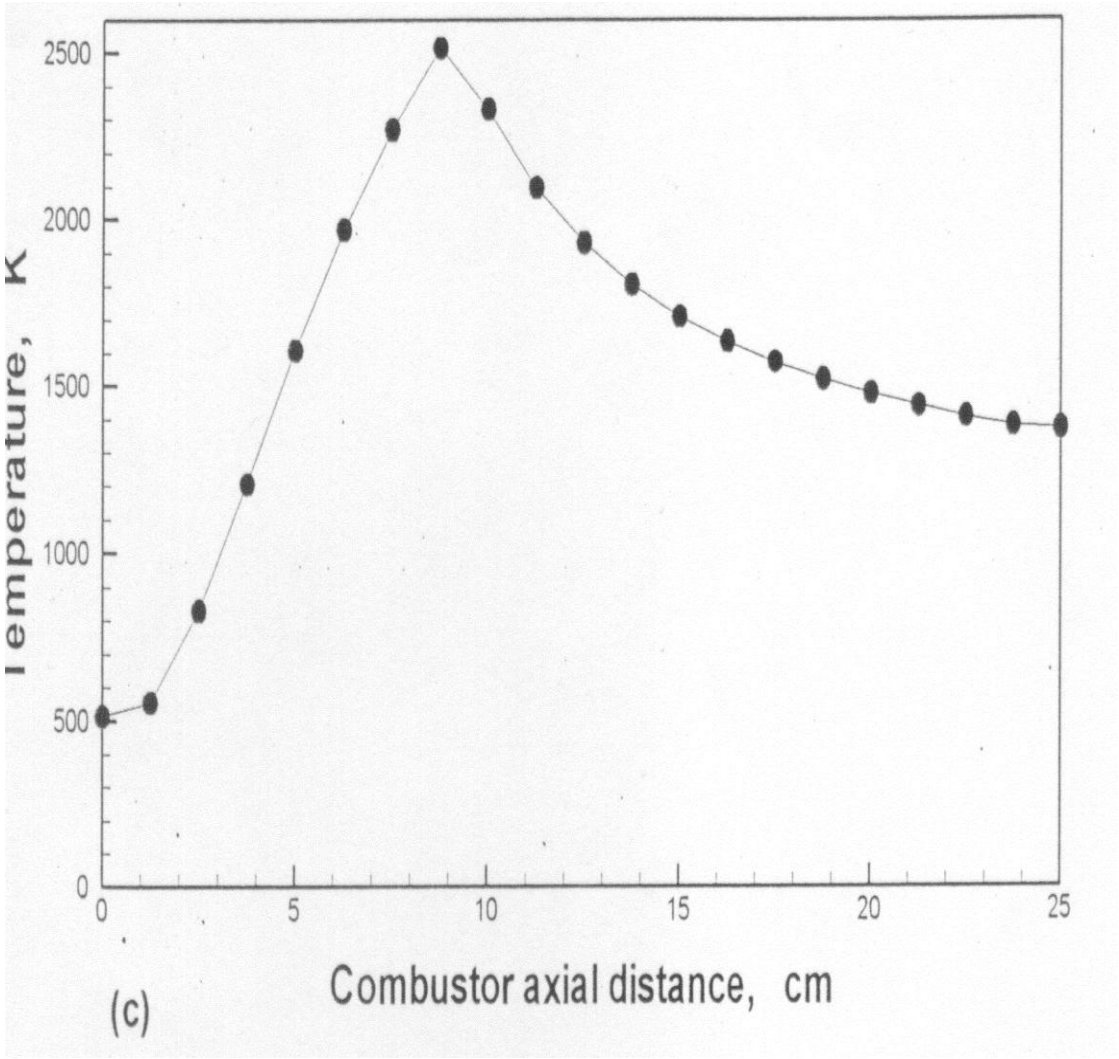

Fig.(6) Temperature Behavior along the Combustion Axis
(c) v_f=0.5 v_o

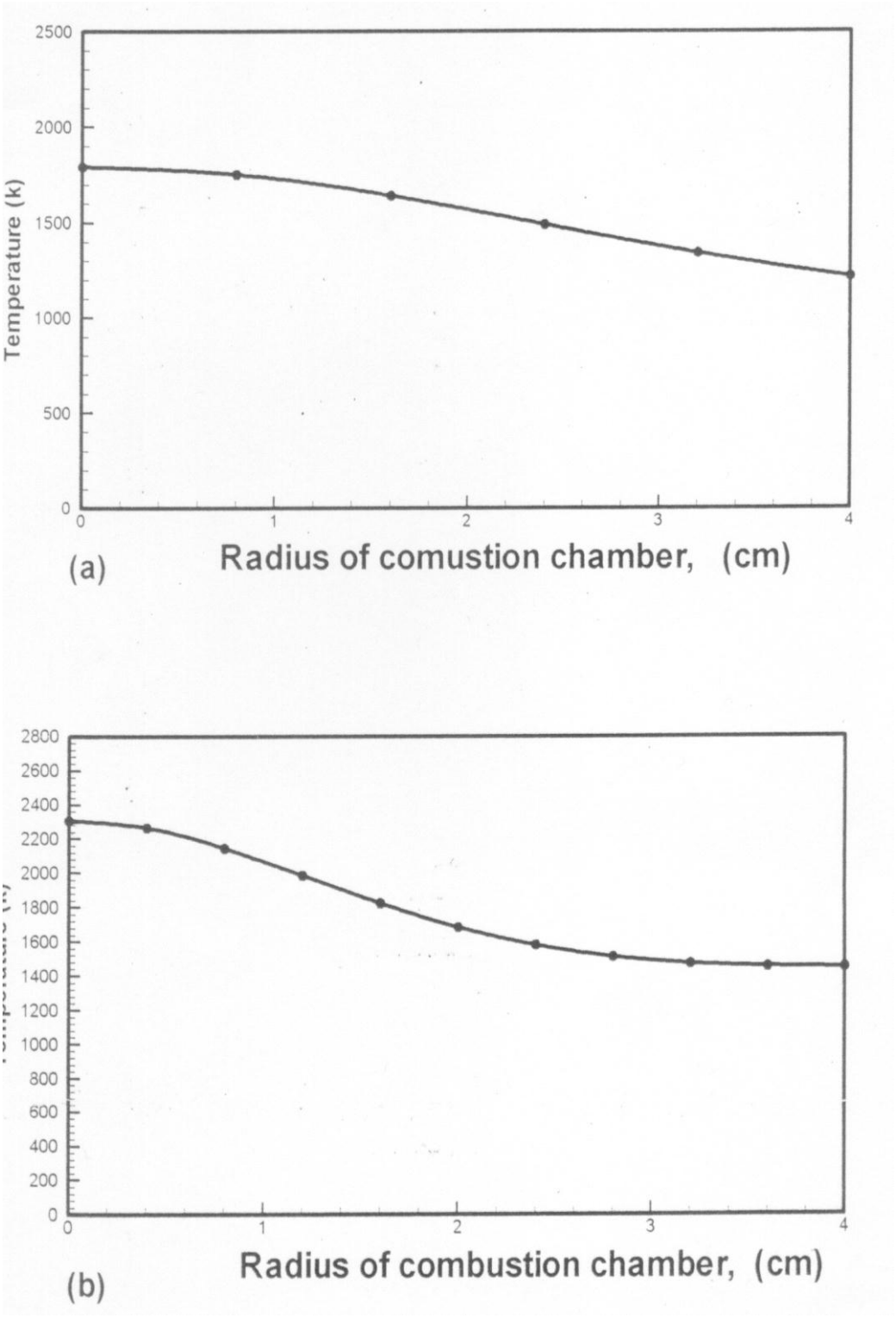

Fig.(7) Temperature Profile at the Exit of Combustion Chamber for (a) $v_f=0.5\ v_o$ (b) $v_f=v_o$

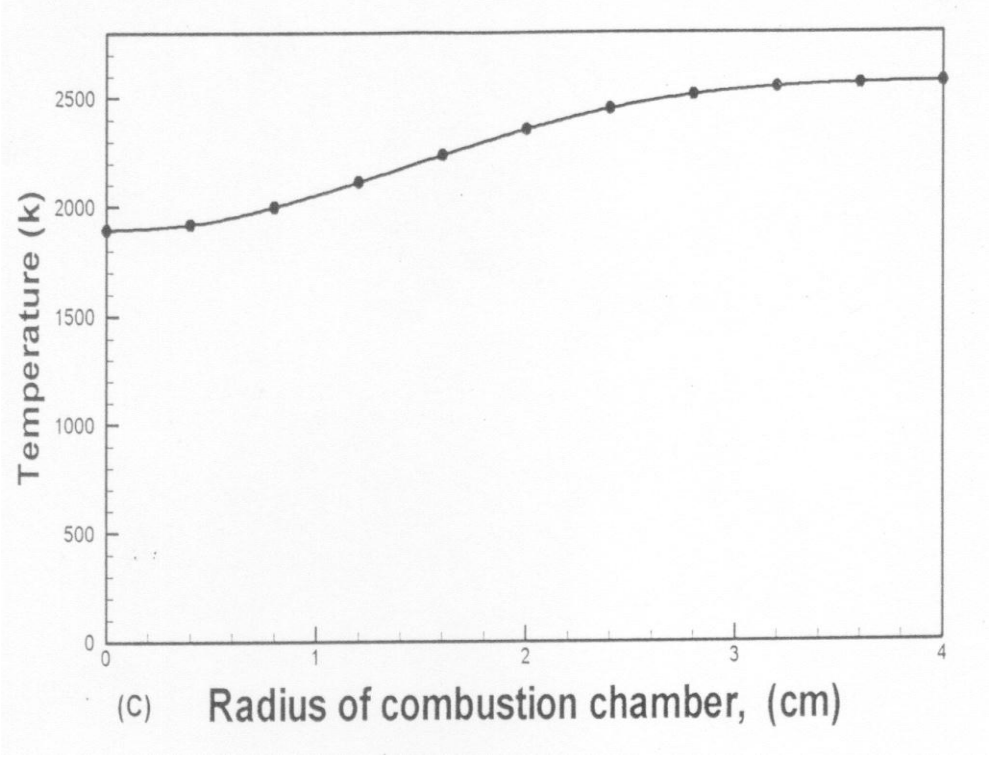

Fig.(7) Temperature Profile at the Exit of Combustion Chamber for $v_f=3v_o$

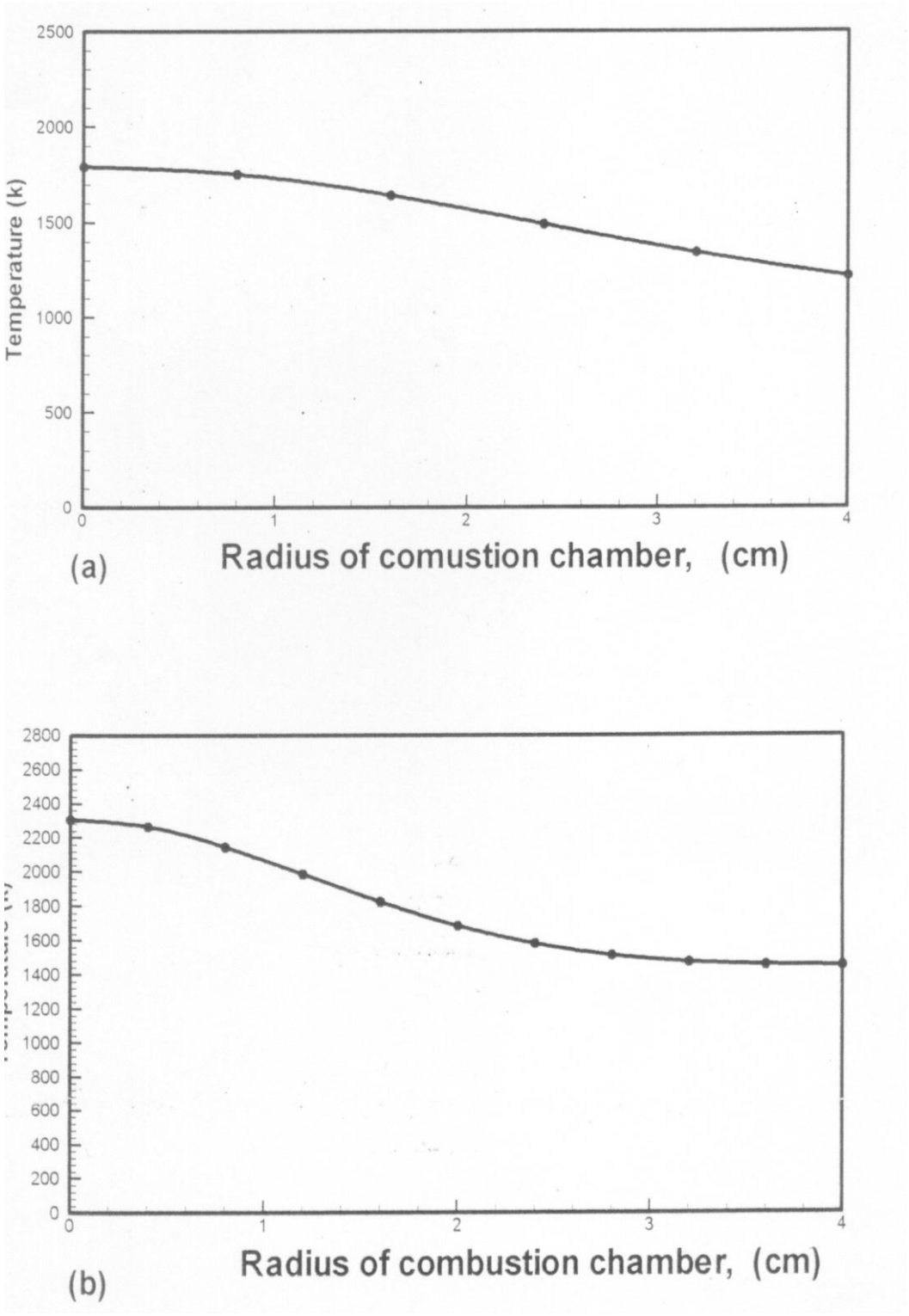

Fig.(8) Temperature Profile at the Exit of Combustion Chamber for (a) $v_f=0.5\ v_o$ (b) $v_f=v_o$

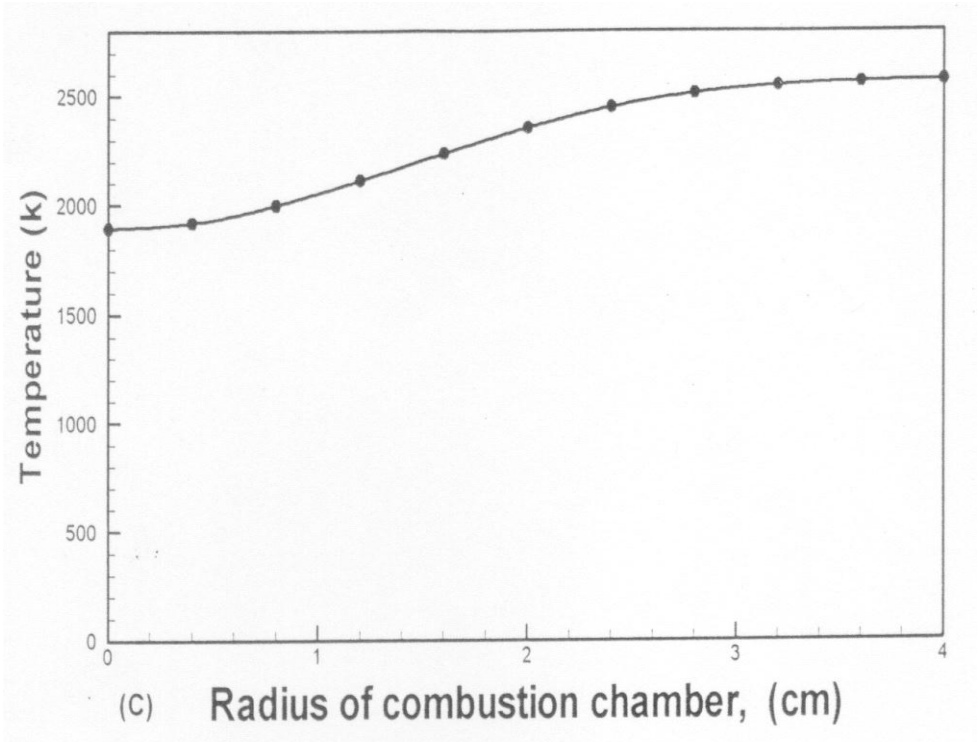

Fig.(8) Temperature Profile at the Exit of Combustion Chamber for $v_f=3v_o$